

# Physical aging of blends of cellulose acetate polymers with dyes and plasticizers

C.J.T. Landry\*, K.K. Lum, J.M. O'Reilly

*Imaging Materials and Media, R&D, Eastman Kodak Company, Rochester, NY 14650-2116, USA*

Received 19 May 2000; received in revised form 11 December 2000; accepted 12 December 2000

## Abstract

A systematic study of physical aging in polymers that have been plasticized by the addition of dyes and polymeric plasticizers is undertaken using the heat capacity as the structural probe. The dyes are actually dye sets and are mixtures of various dyes with slight structural differences, each with a different glass transition temperature ( $T_g$ ). The polymeric plasticizers are low molecular weight polyesters that have low values of  $T_g$ . From experimental results and their analysis, it is shown that aging occurs under ambient temperature conditions most rapidly for the polymer–dye samples that have their  $T_g$  value at 20°C above ambient temperature. The results for these thermorheologically complex blends also indicate that, although the incorporation of the polymeric plasticizers substantially reduces the  $T_g$  of the blend, the distribution of relaxation times is broadened.

Kinetics of aging for the blends are determined using the Tool–Narayanaswamy model for structural relaxation. The fictive temperatures were calculated as a function of annealing temperatures and annealing times in order to assess the effects of storage upon the practical performance of these blends. © 2001 Elsevier Science Ltd. All rights reserved.

*Keywords:* Physical aging; Polymer blends; Polymeric plasticizer

## 1. Introduction

Dye–polymer mixtures are widely used in printing, imaging, and information storage applications. Physical properties, such as the glass transition temperature ( $T_g$ ), greatly affect their performance. Slark has studied the effects of dyes on the  $T_g$  of several polymers [1,2]. The type of interaction between the dye and the polymer affects the magnitude of the change in  $T_g$  with dye concentration. The changes in physical properties with annealing at various temperatures, called physical aging [3–10], are important to the end use of these materials. Hodge [5] has reviewed the successes and shortcomings of the models of physical aging. The Adam–Gibbs [5] interpretation of physical aging in terms of configurational entropy is attractive but does not lead to a more quantitative interpretation of the results. McKenna [11] has outlined broadly the importance of physical aging. There are many examples of physical aging [3]. Physical aging has been used [12–14] as a tool for probing the miscibility or immiscibility in a blend of two polymers whose glass transition temperatures ( $T_g$ ) are within 10–20°C of each other. In this case, it is difficult to

distinguish between a single  $T_g$  (miscible blend) and two distinct  $T_g$  values that are closely spaced (immiscible blend). However, if the two polymers are actually phase separated, they will undergo physical aging at different rates for a specific set of conditions due to their differing molecular structure, and develop very distinct aging peaks (differential scanning calorimetry, DSC) that can be readily resolved.

Ott [15] has found a one to one correlation between the changes in yield strength during physical aging and changes in enthalpy of several polymers. Paul and McCraig [16] have shown that physical aging is responsible for a significant decrease in gas permeability for a polyarylate. They found that physical aging occurs by two distinct and simultaneous mechanisms; one that is thickness dependent and another that is not. Although the importance of physical aging is well documented in mechanical properties [11], and dimensional stability [17], its importance in imaging and information materials has not been studied. Recently, Hutchinson et al. [18] have suggested that the structure dependence of the relaxation time ( $\alpha$ ) should be temperature dependent due to the temperature dependence of the configurational entropy, and may address some weaknesses of the model. Extensive data will be required to fully test this model. Bisquert-Mascarell [19] has suggested that the

\* Corresponding author. Fax: +1-716-477-6498.

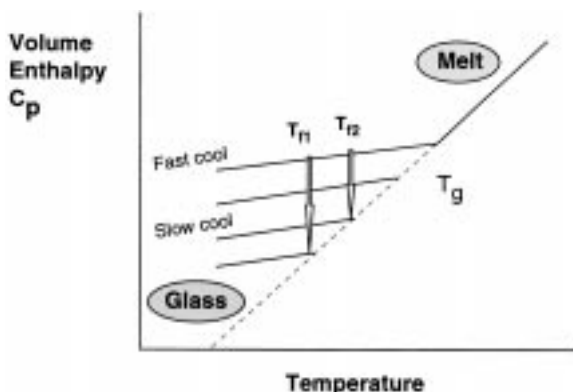
*E-mail address:* christine.landry-coltrain@kodak.com (C.J.T. Landry).

non-linear feature of the model is not necessary to describe structural relaxation. This approach may simplify the analysis and may help to explain the correlation of  $x$  and  $\beta$  frequently observed in experimental data.

A systematic study of physical aging in several mixtures of polymer with dyes and polymers with dyes and plasticizers is undertaken using the heat capacity ( $C_p$ ) as the structural probe. The heat capacity is measured by DSC. The polymers are cellulose acetate polymers. The dye sets and polymeric plasticizers, both with low glass transition temperatures, are intimately miscible with the polymers, and thus depress the glass transition temperature of the cellulose acetate polymer. These measurements were undertaken as part of a study to evaluate the effects of storage upon the practical performance of these blends.

### 1.1. Description of physical aging

In the liquid state, molecular adjustments in packing and free volume to a change in temperature are rapid. However, below the  $T_g$ , these adjustments are much slower. Thus, when an amorphous material is quenched into the glassy state, it is in a non-equilibrium state. As a result of the non-equilibrium nature of the glassy state, all polymers and glasses undergo slow thermodynamic changes (volume, enthalpy, entropy) with time as they spontaneously progress from this metastable state to a lower free energy state when they are stored below their  $T_g$ . These changes occur because the polymer or glass possesses excess volume, entropy, and enthalpy. The approach to equilibrium involves molecules falling into lower energy conformations and into more closely packed regions (lower free volume). This is shown by the schematic below.



The approach to equilibrium is called physical aging and translates directly into changes in physical and mechanical properties (strength, modulus, brittleness) as a result of loss in polymer mobility associated with a decrease in the amount of free volume of these materials. This relaxation in the glassy state observed in volume relaxation and enthalpy relaxation, is referred to as structural relaxation, stabilization, or annealing [3–10].

Physical aging is apparent from the heat capacity curves

in the DSC experiment after the sample has been annealed in the glassy state at temperatures slightly below  $T_g$ . This is also referred to as ‘sub- $T_g$  annealing’. The appearance of an enthalpic overshoot at  $T_g$  after a sample has undergone sub- $T_g$  annealing is characteristic of the DSC trace.

The physical aging process occurs more rapidly as the sub- $T_g$  annealing temperature approaches the  $T_g$ , although the exact rate is also dependent on the polymer type and sample composition.

The Tool–Narayanaswamy (T–N) model for structural relaxation [20–23] incorporates the effects of thermal history through the use of a concept of the fictive temperature ( $T_f$ ). The fictive temperature is the temperature where the glass would come into equilibrium with the liquid. The fictive temperature is a measure of the relaxing part of the enthalpy (expressed in temperature units) and can be viewed as a measure of the degree of departure from equilibrium. The relaxation time of the system increases as  $T_f$  decreases. When the fictive temperature and the actual temperature are the same, the system is in equilibrium. Another way to view the fictive temperature is that the free volume is proportional to the fictive temperature. Lower fictive temperature implies lower free volume. In terms of enthalpy, the fictive temperature is defined as

$$T_f(t) = T_0 + [H(t) - H(\infty)]/\Delta C_p \quad (1)$$

where  $T_0$  is a reference temperature,  $H(t)$  and  $H(\infty)$  are the enthalpy at time  $t$  and at equilibrium, and  $\Delta C_p$  is the change in heat capacity at the glass transition temperature.

Tool found that the relaxation time depends on temperature and fictive temperature and proposed the following equation:

$$\tau = \tau_0 \exp[x\Delta H/RT + (1 - x)\Delta H/RT_f] \quad (2)$$

or

$$\ln \tau(T) = \ln \tau_0 + [x\Delta H/RT + (1 - x)\Delta H/RT_f] \quad (3)$$

where  $\Delta H$  is an activation enthalpy for the relaxation times controlling the structural relaxation,  $R$  is the gas constant,  $\tau_0$  (sometimes denoted  $A$  by other authors) is a characteristic relaxation time, and  $x$  is a constant between 0 and 1.  $x$  is the weighting factor for  $T_f$  and indicates the relative importance of  $T$  and  $T_f$ . When  $x = 1$ , the relaxation is a function of temperature only and when  $x = 0$ , the relaxation time depends only on  $T_f$ . The temperature behavior of the relaxation time constant is described as being Arrhenius in both the actual temperature and fictive temperature.

A knowledge of the parameters in Eq. (2) ( $\tau_0$ ,  $x$ , and  $\Delta H$ ) for a specific property enables the calculation of the dependence of that property, in the glass transition region, on any arbitrary thermal history. The pursuit of this knowledge was the motivation for the present study, thus the choice of utilizing the T–N model over other possible models discussed in Ref. [5].

The T–N model describes the non-exponential character of the structural relaxation with a distribution of relaxation

times that can be both temperature and structure dependent. The relaxation function can be represented by a Williams–Watts [24] function

$$\phi(\tau) = \exp[-(t/\tau)^\beta] \quad (4)$$

where  $\beta$  specifies the breadth of the distribution of relaxation times ( $0 < \beta \leq 1$ ). A value of  $\beta = 1$  indicates a single relaxation time. The lower the value of  $\beta$ , the broader the relaxation time spectrum.

The experimental specific heat data are converted to

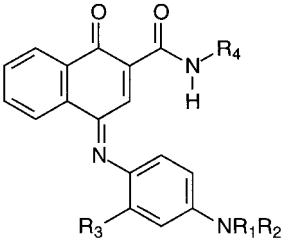
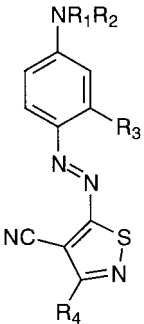
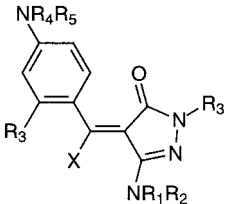
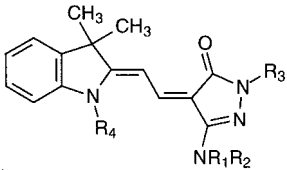
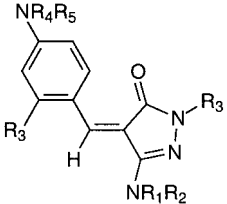
$dT_f/dT$  and analyzed as described previously [25–27]. The change in enthalpy with time–temperature history can be calculated from

$$H(T_f) - H(T_0) = \Delta C_p(T_f - T_0) \quad (5)$$

$$\left. \frac{dT_f}{dT} \right|_T = \left. \frac{[C_p(T) - C_{pg}(T)]}{[C_{p1}(T) - C_{pg}(T)]} \right|_{T/T_f} \quad (6)$$

where  $C_p(T)$  is the experimental specific heat curve of the

Table 1  
Compounds used in blend formulations

Sample	Chemical name	$T_g$ (°C) (onset) <sup>a</sup>	$T_g$ (°C) <sup>a</sup> (midpoint)	
CAP20	Cellulose acetate propionate 482-20 Eastman Chemical Company	141	148	
CAP05	Cellulose acetate propionate 482-05 Eastman Chemical Company	134	142	
Dye set I	 naphthoquinoneimine	45–51	50–54	
Dye set II	 	52–60	54–64	
Dye set III	 isothiazoleazoaniline	 arylidene pyrazolone	31–65	34–67
D429	merocyanine Drapex 429 from Witco Poly(1,3-butylene glycol adipate) $M_w = 4800$ (PS equivalents)	–55	–52	
G25	Paraplex G-25 from C.P. Hall. Polyester sebacate $M_w = 28,000$ (PS equivalents)	No $T_g$ observed	$T_m = -26^\circ\text{C}$ $T_c = -35^\circ\text{C}$	

<sup>a</sup> Measured by DSC at 20°C/min; ranges of  $T_g$  values are indicated for slight variations in dye structure.

aged sample,  $C_{p_g}(T)$  is the glassy specific heat below  $T_g$  (assumed to be linear), and  $C_{p_l}(T)$  is the liquid specific heat above  $T_g$  (assumed to be linear).

$$T_f(T) = T_0 + \int_{T_0}^T dT' \left\{ 1 - \exp \left[ - \left( \int_{T'}^T dT'' / q \tau \right)^\beta \right] \right\} \quad (7)$$

where  $q$  is the heating rate. The activation energy  $\Delta H$  can be calculated from the cooling rate ( $q_c$ ) dependence of the fictive temperature and is evaluated from the DSC heat capacity curves measured on heating.

$$\Delta H/R = T^2 [d \ln q_c / d T_f] \quad (8)$$

Initial values of  $\Delta H$  are obtained and are used in the optimization program to determine the other parameters:  $\ln \tau_0$ ,  $x$ , and  $\beta$ . The  $\ln \tau_0$  and  $\Delta H$  determine the characteristic enthalpic relaxation time.  $\Delta H$  and  $\ln \tau_0$  are not independent parameters.

$T_g$  is defined as the midpoint of the step in the  $C_p$  curve, and is a rate dependent parameter [25]. The relaxation time

at  $T_g$  is defined by  $\tau_g$

$$\ln \tau_g = \Delta H / RT_g + \ln \tau_0 \quad \text{when } T_f = T \quad (9)$$

The physical aging of the polymer–dye blend can be characterized by measuring and analyzing the specific heat curves of the annealed samples as a function of time, temperature, heating and cooling rates. From these data, the fictive temperatures are calculated and the curves are fit by the T–N model from which the parameters  $\Delta H$ ,  $x$ , and  $\beta$ , characteristic of the sample, are obtained.

The primary parameter is the activation energy,  $\Delta H$ , which is determined from the change in  $T_f$  with cooling rate. In general,  $\Delta H$  increases with increasing  $T_g$  as shown for polyesters [28], polycarbonates [29], and indane glasses [30]. For polymers, organic glasses (like dyes), and low  $T_g$  organic liquids (like plasticizers),  $\Delta H$  varies from 100 to 320 kcal/mol as  $T_g$  changes from  $-40$  to  $185^\circ\text{C}$ .

$\Delta H$  of a composite sample will be determined by the  $\Delta H$  of the individual components. If the components are miscible, a single  $\Delta H$  for the sample will govern the relaxation behavior. If the components are not miscible, each immiscible component will relax with its own  $\Delta H$ . Often, the  $C_p$  curve through  $T_g$  is broadened even when all the components are miscible. The parameter  $\beta$ , which is a measure of the breadth of the distribution of relaxation times, will be affected by the distribution of relaxation times of each component. The lower the value of  $\beta$ , the broader the distribution, resulting in the enthalpy recovery curve being smeared out over a wide temperature range. Therefore, a broad distribution of relaxation times can be due to either

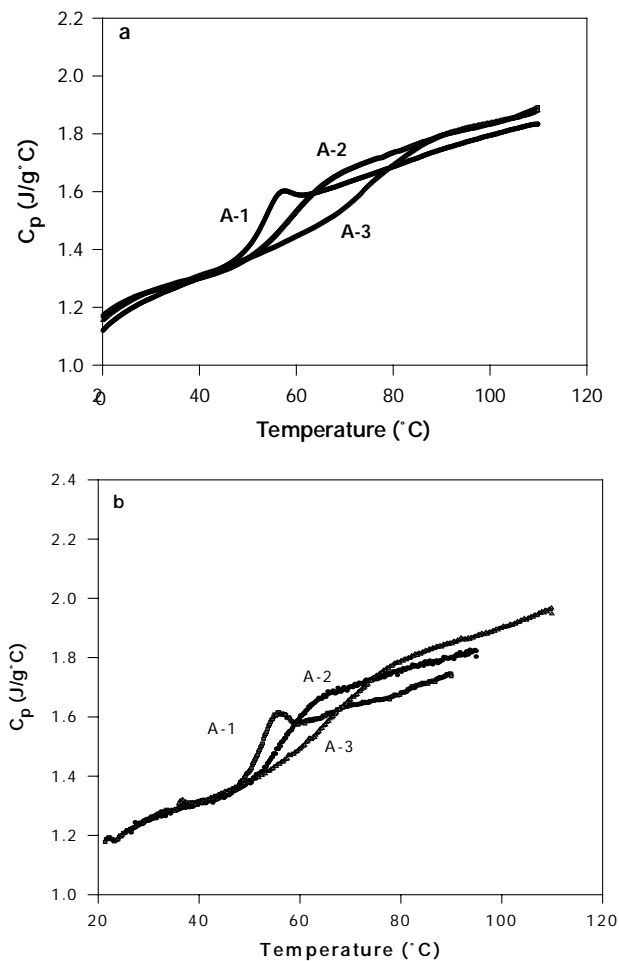


Fig. 1. Heat capacity curves for samples A1–A3, obtained at a heating rate of (a) 20 and (b)  $5^\circ\text{C}/\text{min}$ .

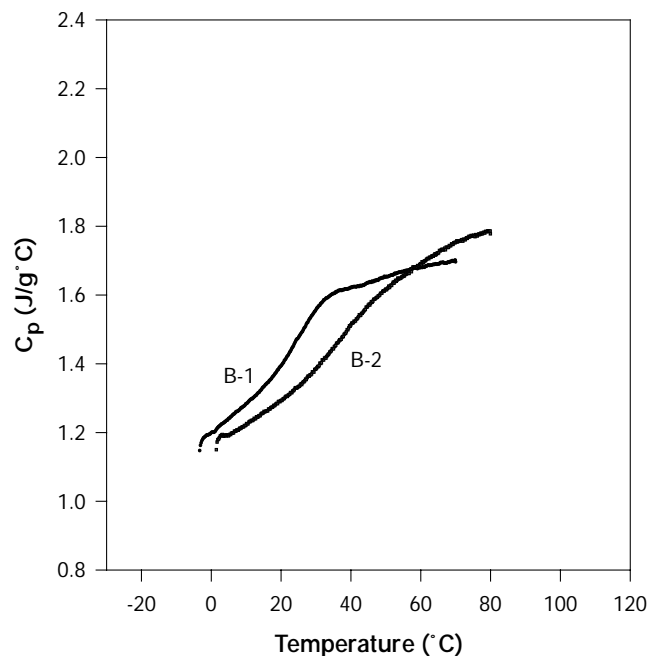


Fig. 2. Heat capacity curves for samples B1 and B2 obtained at a heating rate of  $5^\circ\text{C}/\text{min}$ .

compositional heterogeneity or heterogeneity in physical aging, or both. Multicomponent systems can give apparent low values of  $\beta$ , confounding its interpretation. Because the samples discussed herein consist of a binder polymer, dye molecules, and plasticizers, all these components will contribute to the physical aging parameters in a complex manner. Correlations also exist between  $x$  and  $\beta$ , which further complicate more detailed interpretation of physical aging phenomena. A good discussion on how  $x$  and  $\beta$  affect the relaxation curve shapes can be found in Ref. [3].

In the present work, the effects of dyes and polymeric plasticizers on physical aging were examined. The samples are single-phase blends of a polymeric binder, cellulose

acetate propionate (CAP), with a mixture of dyes and in some, of plasticizers. Although the  $T_g$  of CAP is high (148°C), the dyes have lower  $T_g$  values and, at high dye content, this results in a blend that has a  $T_g$  that is only slightly higher than ambient temperature. Thus, physical aging of the blend occurs relatively rapidly under ambient conditions. During this process, volume relaxation occurs.

The T–N physical aging model [20–23] is used to model thermal data obtained via DSC in order to predict aging behavior for current blends and compositions incorporating polymeric plasticizers. These data are used to calculate the effect of practical thermal histories on the properties of these mixtures.

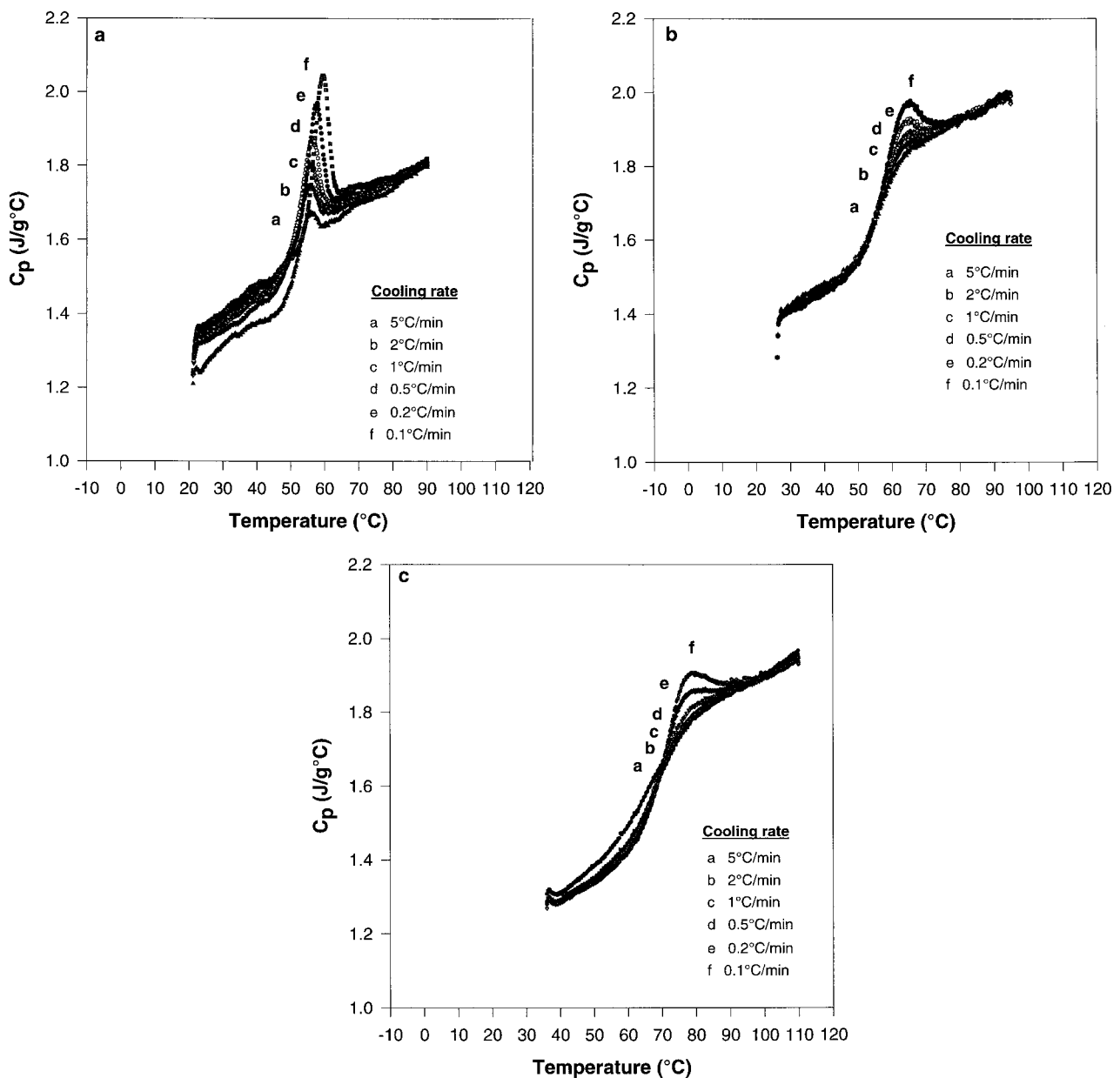


Fig. 3. Heat capacity curves, obtained at a heating rate of 5°C/min after cooling at the rate indicated, for samples (a) A1, (b) A2, and (c) A3.

## 2. Experimental

### 2.1. Chemicals

Cellulose acetate propionates were obtained from Eastman Chemical Company. CAP482-20 is a higher molecular weight than CAP482-05. Most samples contained either pure CAP482-20 or CAP482-20 with minor amounts of CAP482-05. Both have an acetyl content of 2.5 wt% and a propionyl content of 45 wt%. The dyes were prepared in house and are listed as dye classes. Polymeric aliphatic polyester plasticizers D429 (from Witco) and G25 (from C.P. Hall) are viscous liquids with polystyrene equivalent weight average molecular weights of 4810 and 27,000, respectively, as determined by size exclusion chromatography (SEC). Information on all these, along with their glass transition temperatures ( $T_g$ ) can be found in Table 1. Methylene chloride (DCM) was used as received.

### 2.2. Preparation of samples for DSC

Solutions of each blend formulation were prepared by dissolving the components (dyes, CAP, and plasticizers) in DCM. These solutions were stirred overnight and cast into Teflon molds and dried under vacuum for several days. The films were further dried using moderate temperatures under vacuum to ensure full removal of the solvent, and 8–15-mg samples were cut from these films for DSC measurements. All samples were refreshed by heating to temperatures above  $T_g$  before commencing the aging experiments. The samples studied are listed in Table 2.

### 2.3. DSC measurements

DSC was performed in a nitrogen atmosphere on a Perkin–Elmer DSC-7 calorimeter with a 7 Series/UNIX thermal analysis program. The heating rates used were either 5 or 20°C/min, as indicated. The  $T_g$  is taken as the midpoint of the change in heat capacity with temperature. The onset  $T_g$  of this change is also noted.

Cooling experiments were performed to obtain values for  $\Delta H$ . The sample was heated to above  $T_g$ , held for 2 min, cooled to below  $T_g$  at a controlled rate ( $q_c$ ), then heated at a rate of 5°C/min through the  $T_g$ .  $q_c$  is varied from 0.1 to 5°C/min.  $T_f$  is calculated for each cooling rate by drawing the slopes of the  $C_p$  curves above and below  $T_g$  and applying Eq. (6) to calculate  $dT_f/dT$ . These calculations are done automatically by the DSC7 software.  $\Delta H$  is calculated from the slope of a plot of  $\ln q_c$  versus  $1/T_f$ , or from a plot of  $T_f$  versus  $\ln q_c$ . Cooling experiments were not performed for the initial 20°C/min data, thus a fixed value of 100 kcal/mol was assumed for  $\Delta H$  for further calculations.

The annealing experiments were performed by heating the samples to above  $T_g$ , cooling at a rate of  $q_c$  (either 5 or 20°C/min) to the annealing temperature  $T_a$  (5–30°C below  $T_g$ ), and holding at that temperature for

the annealing time  $t_a$ . This was followed by cooling at  $q_c$  to about 40°C below  $T_g$ , holding for 2 min and heating at  $q_h$  (either 5 or 20°C/min) through the  $T_g$ . This procedure was repeated for several annealing times and temperatures. The resulting curves are then fit to the T–N model by an optimization procedure. Best-fit values for  $x$ ,  $\beta$ , and  $\ln \tau_0$  are determined. The value of  $\Delta H$ , determined from the cooling experiments, remains fixed during the fitting.

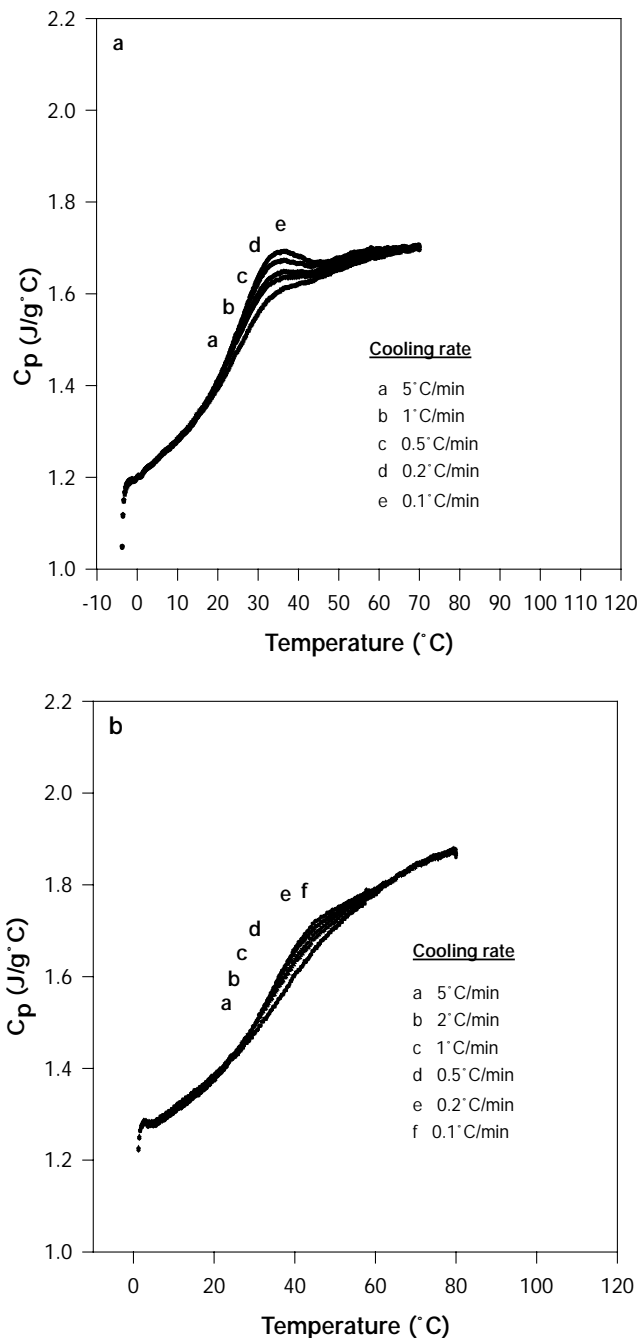


Fig. 4. Heat capacity curves, obtained at a heating rate of 5°C/min after cooling at the rate indicated, for samples (a) B1 and (b) B2.

Table 2  
Composition and glass transition temperatures of blend formulations

Sample	Total dyes (wt%)	Total plasticizer (wt%)	$T_g$ (°C) (onset) (5°C/min)	$T_g$ (°C) (midpoint) (5°C/min)	$T_g$ (°C) (onset) (20°C/min)	$T_g$ (midpoint) (20°C/min)
A1	62.4 (Dye set I)	0	48	51	46	49
A2	48.2 (Dye set II)	0	52	56	50	58
A3	42.6 (Dye set III)	0	58	68	65	74
B1	55.2 (Dye set I)	7.7 (G25)	19	26	17	28
B2	34.6 (Dye set III)	11.9 (D429)	27	40	22	42

### 3. Results

Table 2 shows the measured values of  $T_g$  of each formulation. These were obtained from samples that were heated to above  $T_g$ , quenched to below  $T_g$  and immediately heated through  $T_g$  without annealing. A slight difference in  $T_g$  was obtained depending on the heating rate because the glass transition temperature is a rate dependent quantity. The heat capacity curves are compared in Figs. 1 and 2.

Figs. 3(a)–(c) and 4(a) and (b) show the resulting DSC curves for samples A1–A3, B1 and B2 obtained from the cooling experiments, all at 5°C/min heating rate. The development of excess enthalpy is different for each sample. In Fig. 3(a), sample A1 rapidly develops specific heat overshoots, indicating rapid aging. At the other extreme, almost no structure develops in sample B2 (Fig. 4(b)) that contains D429 plasticizer. The activation energy,  $\Delta H$ , is calculated from the slope of a plot of  $\ln q_c$  against  $1/T_f$ , as shown in Fig. 5 for sample A2.

Figs. 6(a)–(c) and 7(a) and (b) show the series of annealing experiments for each sample. The annealing temperatures and times were chosen as to maximize the amount of aging that would occur during the experiments. Typically, chosen annealing temperatures are 10–30°C below the midpoint of  $T_g$ . Each of these experimental curves is fit to the T–N model and values for  $x$ ,  $\beta$ , and  $\ln \tau_0$  are determined. The value of  $\Delta H$ , determined from

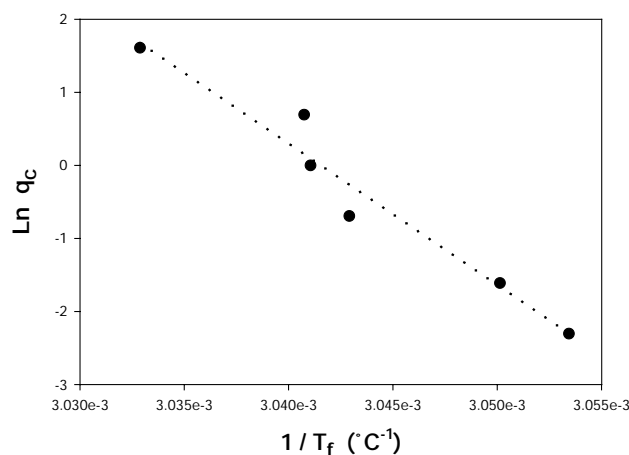


Fig. 5. Cooling rate dependence of the fictive temperature for sample A2.

the cooling experiments, remains fixed during the fitting. Typical fits of the theory to the data are shown in Fig. 8. These represent fairly good fits to the data. In many cases, however, the fit is not as good. This is primarily a result of the broadness of the experimental curves. Broad distributions are not always thermorheologically simple and indicate that all the relaxation times are not changing equally with temperature. The experimental curves are broad because of the multicomponent composition of the samples and because the cellulose acetates themselves have broad glass transitions. Average values were calculated (listed in Table 3) from the annealing data only (omitting outliers) and used to calculate predicted fictive temperature behavior at longer times and various annealing temperatures.

### 4. Discussion of the results

As evident from the DSC curves in Fig. 1, the glass transition temperatures are very different for samples A1–A3. This is primarily a result of the differing values of  $T_g$  of each dye, and the relative amounts of dye found in each sample. The DSC curves obtained at 5 and 20°C/min are very similar. The incorporation of the polymeric plasticizer lowers the  $T_g$  of the sample even more and alters its aging characteristics. Two polymeric plasticizers were utilized, D429 and G25. These are both aliphatic polyesters and their characterization and  $T_g$ s are listed in Table 1. There is some precedence in mixing aliphatic polyesters with cellulose acetates. Buchanan et al. [31,32] have demonstrated miscibility between several cellulose acetates and aliphatic polyesters. For example, CA398-30, CAP482-20, and CAP141-20 were found to be miscible (melt blended) with poly(ethylene glutarate) and poly(ethylene succinate). Miscibility between the cellulosic polymer and the polymeric plasticizer is important in order to keep the already complex mixture as homogeneous as possible.

Table 3 compares the best-fit values for the parameters for the different samples and for the two different experimental conditions used (5 and 20°C/min heating rates). Initially, the cooling runs were also analyzed to extract values for the parameters. However, these either yielded values that were very close to those obtained from the annealing data, or were not realistic. Therefore, for consistency it was

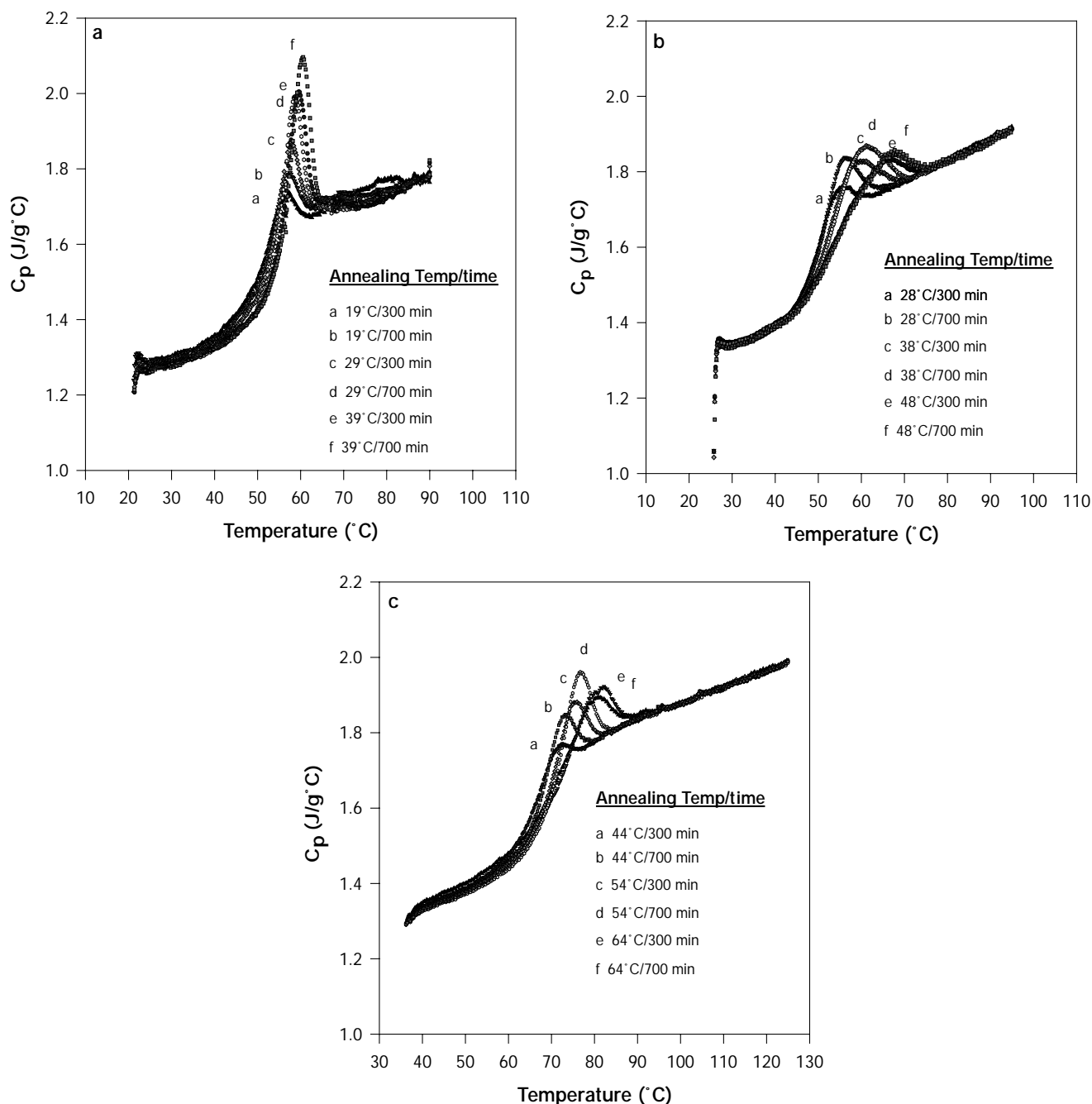


Fig. 6. Heat capacity curves, obtained at a heating rate of 5°C/min after annealing at the specified temperature for the specified time, for samples (a) A1, (b) A2, and (c) A3.

decided that only parameter values ( $\ln \tau_0$ ,  $x$ , and  $\beta$ ) obtained from the annealing DSC data should be used.

The parameter  $\beta$  characterizes the broadness of the distribution of relaxation times. Typical values of  $\beta$  are in the range of 0.3–0.5, indicating broader relaxation spectra, perhaps because of the multitude of constituents in each sample. Sample A1 exhibits a much higher value of  $\beta$  than the others, indicating narrower relaxation spectra. The parameter  $x$  determines how strongly the relaxation times depend upon  $T_f$  [Eq. (2)]. Small values of  $x$  (0.1–0.3) lead to strong dependence on  $T_f$  and large peak heights.

Values of  $x = 0.3$  to 0.6 are typical and give modest overshoots. Larger values of  $x$  are atypical. The relaxation time at  $T_g$ ,  $\ln \tau_g$ , is determined by the value of  $\ln \tau_0$  [Eq. (9)]. Low values of  $\ln \tau_g$  (from 2 to 5) lead to faster relaxation times. Typical values of  $\ln \tau_g$  are from 5 to 8. Long relaxation times at  $T_g$  greater than 8 are observed in slow relaxing systems like crosslinked epoxides or semi-crystalline polymers. The uncertainty in  $x$  and  $\beta$  is typically  $\pm 0.05$ . In many cases  $x$  and  $\beta$  are correlated. For these reasons only significant changes are interpreted. An examination of the sharpness and temperature dependence of the enthalpy curves



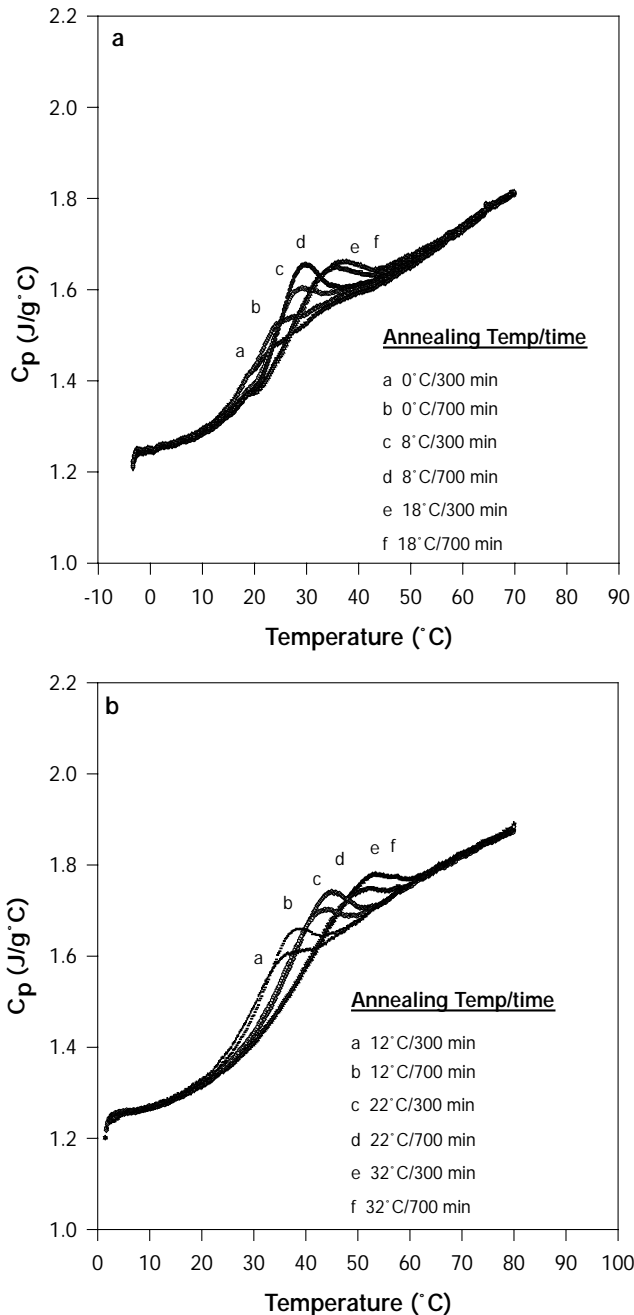


Fig. 7. Heat capacity curves, obtained at a heating rate of 5°C/min after annealing at the specified temperature for the specified time, for samples (a) B1 and (b) B2.

from the cooling and annealing experiments suggest that of samples A1–A3, sample A1 relaxes fastest. Sample B2 relaxes more slowly than do the others. This behavior is reflected in a general way by the calculated values found in Table 3.

Fig. 9(a) shows the predicted (obtained from the 5°C data, using the values in Table 3) dependence of  $T_f$  on annealing temperature for a 30-day aging time. The minimum of the curves represents the temperature at which the particular sample reaches its lowest  $T_f$  (ages most rapidly). In each

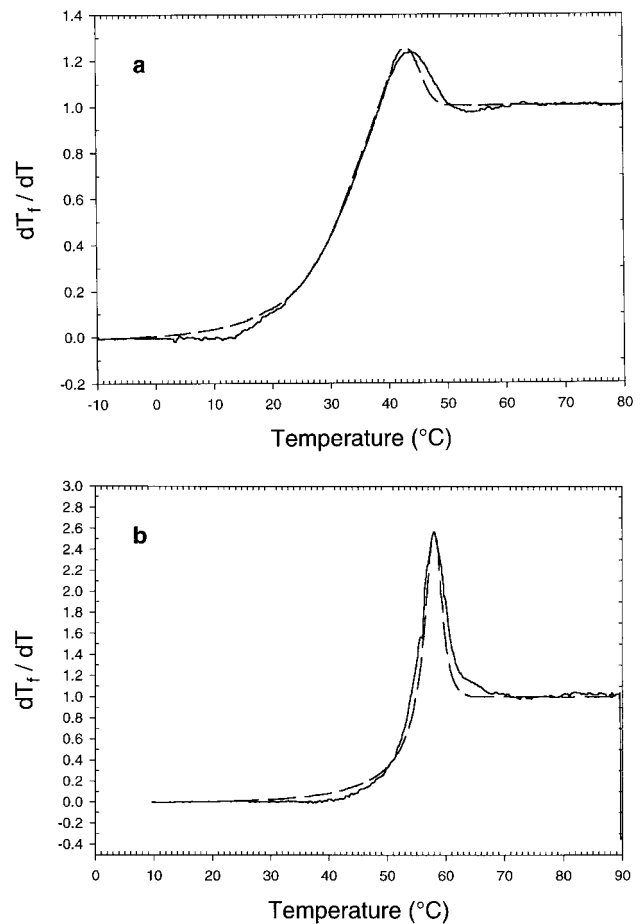


Fig. 8. Typical theoretical fits (dashed line) to the annealing data (solid line) for (a) sample B2 annealed at 22°C/700 min, and (b) sample A1 annealed at 29°C/700 min.

case, the minimum occurs at approximately 20°C below the value of  $T_g$  (midpoint) measured for the sample. A curve obtained from the 5°C data cannot be compared exactly to the curve obtained from the 20°C data unless all the fitting parameters ( $x$ ,  $\beta$ ,  $\tau_0$ ,  $\Delta H$ ) are identical, which generally is not the case. Although the minimum values in  $T_f$  differ as expected, both sets of data (5 and 20°C) show similar behavior and the minima occur near the same temperature. The curves illustrate that ambient temperature aging is occurring at very different rates for each of the three samples A1–A3. The corresponding predicted dependence of  $T_f$  on annealing temperature for the plasticized samples is shown in Fig. 9(b). The lower minima in the fictive temperature curve obtained for sample B1 is a result of the  $T_g$  being slightly lower than that of B2. The curves for samples B1 and B2 are much shallower than those for samples A1–A3, reflecting the decrease in the magnitude of the change in  $T_f$  as the incorporation of the plasticizer broadens the glass transition and diminishes the size of the aging peaks.

Fig. 10 shows the predicted dependencies of  $T_f$  on annealing time at various annealing temperatures for two

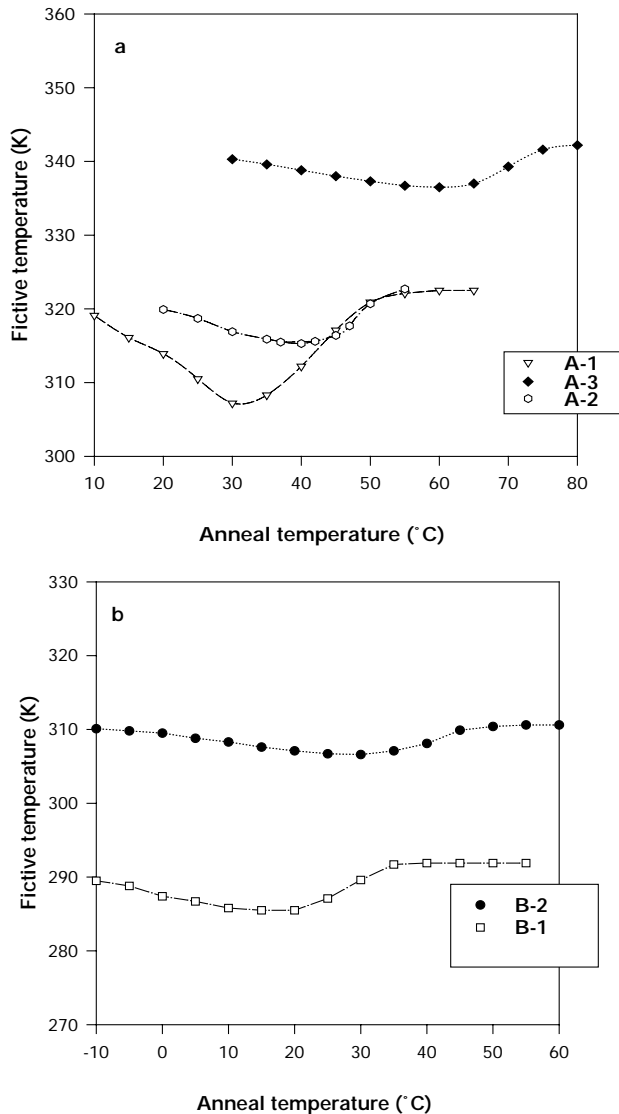


Fig. 9. Predicted dependence of the fictive temperature on annealing temperature for a 30-day aging for samples (a) A1–A3, and (b) B1 and B2; the 5°C/min data was utilized.

different samples. The curves are taken out to very long times (>1 year) for illustrative purposes only. One must remember, however, that the model does not extrapolate to long times very accurately. Data should be taken over the experimental  $T$  and  $t$  range of interest. Extrapolation of the results by more than three times the longest experimental aging time is very risky. However, a qualitative view of how the sample will change within several months at ambient keeping, and for shorter time preconditioning (or annealing) is useful. As shown in Fig. 10(a), these predictions demonstrate that annealing at 38°C for a few days will bring sample A1 into a much lower ( $T_f$ ) state (more stable) than it would reach under ambient conditions over the same time period. However, for longer annealing times, greater than about a month for example, ambient conditions would lead to a more stable state.

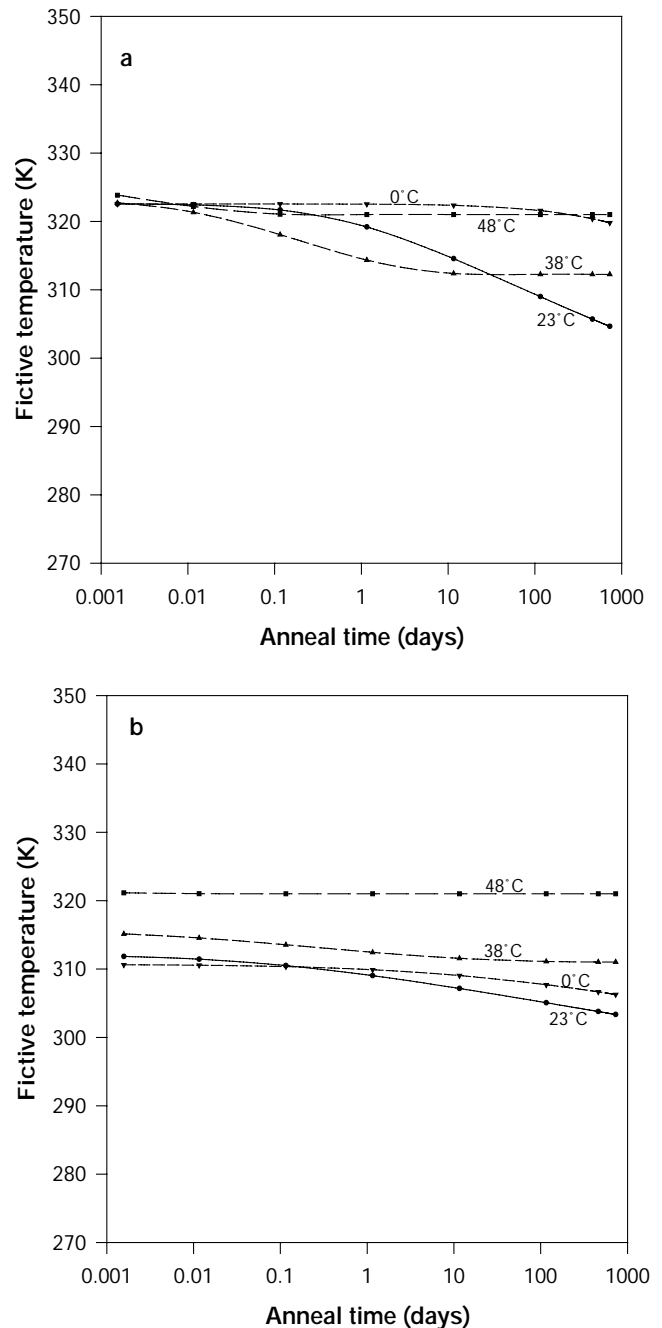


Fig. 10. Predicted dependence of the fictive temperature on annealing time at various temperatures for samples (a) A1 and (b) B2; the 5°C/min data was utilized.

The behavior of the plasticized samples is illustrated in Fig. 10(b) by that of sample B2. Once again the predictions are taken out to very long times for illustrative purposes. The behavior of these samples with time is different from that of the unplasticized blend samples A1–A3. Almost no change in  $T_f$  is observed out to very long keeping times at temperatures slightly above ambient, and small changes are observed at 0 and 23°C. However, these changes are much less pronounced than those predicted for samples A1–A3.

Table 3  
Summary of fitting parameters from annealing data

Donor	$\Delta H$ (cal/mol) <sup>a</sup>	$-(\ln \tau_0)$	$x$	$\beta$	$\ln \tau_g^b$
A1					
20°C/min data	$[1.0 \times 10^5]$	151	0.45	0.70	4.3
5°C/min data	$1.1 \times 10^5$	165	0.52	0.61	4.8
A2					
20°C/min data	$[1.0 \times 10^5]$	145	0.50	0.44	6.1
5°C/min data	$1.7 \times 10^5$	257	0.41	0.37	1.4
A3					
20°C/min data	$[1.0 \times 10^5]$	142	0.75	0.62	2.1
5°C/min data	$2.4 \times 10^5$	345	0.28	0.30	6.9
B1					
5°C/min data	$1.5 \times 10^5$	250	0.31	0.30	0.84
B2					
5°C/min data	$1.5 \times 10^5$	235	0.40	0.22	4.6

<sup>a</sup> Cooling runs were not performed on the 20°C/min data; thus  $\Delta H$  was assumed to be 100 kcal/mol and fixed for the analyses.

<sup>b</sup> Using midpoint value for  $T_g$  obtained at 20 and 5°C/min, respectively.

For these samples, that have lower  $T_g$ , annealing temperatures of 38 and 48°C are within the  $T_g$  region, thus  $T_f$  will not go lower than the annealing temperature. These samples are in equilibrium because  $T > T_g$ . At the lower annealing temperatures (0–23°C), structural recovery is relatively slow, as seen from the cooling experiments.

Although it is more desirable to perform the DSC experiments at the slowest rates possible to achieve maximum precision and a closer proximity to equilibrium [20], the above analysis reveals that very low rates tend to compress the effects caused by loss in signal; the fictive temperature does not vary as much with  $q_c$  as it does at higher rates. The 5°C/min predictions do not really distinguish the behavior of samples A1–A3 as well as the 20°C/min predictions. This is further compounded by the complexity of the formulations. At the higher rates, differences between the behavior of these samples were more obvious and illustrative. The data taken at 20°C/min are self-consistent and qualitatively similar to those taken at 5°C/min, and have better sensitivity. Thus, in this case, it appears that the higher rates can be used to acquire more practical, preliminary information. The value of  $x$  has been observed to be artificially low for higher heating rates. For this reason low heating rates are preferred [26]; however, sensitivity increases with heating rate. Initial measurements were made at 20°C/min, and later measurements were performed at rates of 5°C/min.

The thermal data discussed above show how the properties of samples A1–A3 will change with time and how the lowering of their  $T_g$  by the addition of polymeric plasticizers has altered this response. In addition to lowering the  $T_g$ , the addition of plasticizer along with some changes in the overall composition of the polymer–dye blends has changed the distribution of relaxation times. This alters the thermal aging behavior.

## 5. Conclusions

Modeling of the complex aging behavior of polymer–dye blends was performed using the multiparameter T–N description. The rate of aging is strongly influenced by the location of the  $T_g$  relative to the annealing temperature. The primary controller of the relaxation time (and aging) is  $T_g$ , while the other factors ( $\tau_0$ ,  $x$ ,  $\beta$ ) only modify  $T_g$  effects. A change in  $T_g$  by 2–3°C can change the relaxation time by a factor of 10 [33]. Sample A1 relaxes faster than A2 or A3, as seen by the large sharp enthalpy relaxation peaks. This could be due to the higher mobility of the dye or the higher concentration of dye in the sample. Although the  $T_g$  values are lower for the plasticized samples (B series) all these relax slower than the unplasticized samples, as indicated by broad enthalpy recovery curves. Sample B2 is particularly slow. This behavior may be attributed to the replacement of more-mobile dye molecules by the less-mobile polymeric plasticizer molecules.

Amongst the unplasticized blends, sample A1 relaxes fastest and sample A3 relaxes slowest. These conclusions are supported by the observation from the cooling and annealing enthalpic behavior and the observation that  $T_f$  changes most with cooling rate for A1.

The different plasticized samples have similar aging behavior. Differences are subtle. They show slower aging (low enthalpy recovering peaks seen in cooling experiments) than sample A1. However, they do not change with time primarily because of the lower  $T_g$  values for each and their proximity to room temperature.

As shown herein, the complex nature of the aging phenomenon in multicomponent systems does not allow for simple evaluation, analysis, or absolute prediction of long-term aging properties. However, reasonable qualitative and realistic predictions can be made.

In order to make more quantitative predictions for multicomponent systems, one would like to know the T–N parameters for the individual components. However, knowledge of those parameters is not sufficient to predict the behavior of a multicomponent blend without an improved model, which would more accurately predict long-term behavior.

## Acknowledgements

The authors would like to thank Ms Linda Franklin, Ms Alena Sochor, and Mr Maurice Gray for their valuable contributions to this work.

## References

- [1] Slark AT. Polymer 1997;38:4477.
- [2] Slark AT. Polymer 1999;40:1935.
- [3] Struik LCE. Physical aging of amorphous polymers and other materials. Amsterdam: Elsevier, 1978.
- [4] Petrie SEB. In: Baer E, Radcliffe SV, editors. Polymeric materials: relationships between structure and mechanical behavior. Metals Park, OH: American Society of Metallurgists, 1975.

- [5] Hodge IM. *J Non-Cryst Solids* 1994;169:211.
- [6] Hodge IM, Berens AR. *Macromolecules* 1981;14:1598.
- [7] Hodge IM. *Macromolecules* 1986;19:936.
- [8] Hodge IM, Berens AR. *Macromolecules* 1986;18:1980.
- [9] Hodge IM, Berens AR. *Macromolecules* 1987;20:2897.
- [10] Pannhorst W. *Solid State Ionics* 1998;105:271.
- [11] McKenna G, Arnold-McKenna C. *J Res Natl Inst Stand Technol* 1993;98:523.
- [12] Jorda R, Wilkes GL. *Polym Bull* 1988;20:479.
- [13] Bosma M, ten Brinke G, Ellis TS. *Macromolecules* 1988;21:1465.
- [14] Grooten R, ten Brinke G. *Macromolecules* 1989;22:1761.
- [15] Ott K. *Colloid Polym Sci* 1980;258:995.
- [16] Paul DR, McCraig MS. *Polymer* 2000;41:629.
- [17] Schrader R, Carroll J. US patent 4,141,735, 1979.
- [18] Hutchinson JM, Montserrat S, Calventus Y, Cortes P. *Macromolecules* 2000;33(14):5252.
- [19] Bisquert-Mascarell J, Garcia-Belmonte G. *J Chem Phys* 2000;113(12):4965.
- [20] Tool AQ. *J Res* 1945;34:199.
- [21] Tool AQ. *J Am Chem Soc* 1946;29:240.
- [22] Narayanaswamy OS. *J Am Ceram Soc* 1971;54:491.
- [23] Scherer GW. *Relaxation in glasses and composites*. New York: Wiley, 1986.
- [24] Williams G, Watts DC. *Trans Faraday Soc* 1970;66:80.
- [25] Moynihan CT, Eastal AJ, DeBolt MA, Tucker J. *J Am Ceram Soc* 1976;59:12.
- [26] O'Reilly JM, Hodge IM. *J Non-Cryst Solids* 1991;451:130.
- [27] Tribone JJ, O'Reilly JM, Greener J. *Macromolecules* 1986;19:1732.
- [28] O'Reilly JM. *J Polym Sci Polym Phys* 2000;38:495.
- [29] O'Reilly JM, Lyng RJ. Submitted for publication.
- [30] Hodge IM, O'Reilly JM. *J Phys Chem* 1999;103:4171.
- [31] Buchanan CM. US patent 5,292,783, 1994.
- [32] Buchanan CM, Gedon SC, White AW, Wood MD. *Macromolecules* 1993;26:2963.
- [33] Ferry JD. *Viscoelastic properties of polymers*. 3rd ed. New York: Wiley-Interscience, 1980 (chap. 11).